Self-referenced composite Fabry-Pérot cavity vapor sensors

Karthik Reddy[1,2,3] and Xudong Fan[1,3,*]

[1]*Department of Biomedical Engineering, University of Michigan, 1101 Beal Ave. Ann Arbor, Michigan 48109,USA*
[2]*Department of Electrical Engineering and Computer Science, University of Michigan, 1301 Beal Ave. Ann Arbor, Michigan 48109, USA*
[3]*Center for Wireless Integrated Microsensing and Systems, University of Michigan, Ann Arbor, Michigan 48109, USA*
*xsfan@umich.edu

Abstract: We develop a versatile, self-referenced composite Fabry-Pérot (FP) sensor and the corresponding detection scheme for rapid and precise measurement of vapors. The composite FP vapor sensor is formed by etching two juxtaposed micron-deep wells, with a precisely controlled offset in depth, on a silicon wafer. The wells are then coated with a vapor sensitive polymer and the reflected light from each well is detected by a CMOS imager. Due to its self-referenced nature, the composite FP sensor is able to extract the change in thickness and refractive index of the polymer layer upon exposure to analyte vapors, thus allowing for accurate vapor quantitation regardless of the polymer thickness, refractive index, and light incident angle and wavelength. Theoretical analysis is first performed to elucidate the underlying detection principle, followed by experimental demonstration at two different incident angles showing rapid and consistent measurement of the polymer changes when the polymer is exposed to three different analytes at various concentrations. The vapor detection limit is found to be on the order of a few pico-grams (~100 ppb)

References and links

1. G. Gauglitz, A. Brecht, G. Kraus, and W. Mahm, "Chemical and biochemical sensors based on interferometry at thin (multi-) layers," Sens. Actuators B Chem. **11**(1-3), 21–27 (1993).
2. D. Reichl, R. Krage, C. Krumme, and G. Gauglitz, "Sensing of volatile organic compounds using a simplified reflectometric interference spectroscopy setup," Appl. Spectrosc. **54**(4), 583–586 (2000).
3. J. Liu, Y. Sun, and X. Fan, "Highly versatile fiber-based optical Fabry-Pérot gas sensor," Opt. Express **17**(4), 2731–2738 (2009).
4. J. Liu, Y. Sun, D. J. Howard, G. Frye-Mason, A. K. Thompson, S.-J. Ja, S.-K. Wang, M. Bai, H. Taub, M. Almasri, and X. Fan, "Fabry-Pérot cavity sensors for multipoint on-column micro gas chromatography detection," Anal. Chem. **82**(11), 4370–4375 (2010).
5. C. Martínez-Hipatl, S. Muñoz-Aguirre, G. Beltrán-Pérez, J. Castillo-Mixcóatl, and J. Rivera-De la Rosa, "Detection of volatile organic compounds by an interferometric sensor," Sens. Actuators B Chem. **147**(1), 37–42 (2010).
6. K. Reddy, Y. Guo, J. Liu, W. Lee, M. K. Khaing Oo, and X. Fan, "On-chip Fabry-Pérot interferometric sensors for micro-gas chromatography detection," Sens. Actuators B Chem. **159**(1), 60–65 (2011).
7. K. Reddy, Y. Guo, J. Liu, W. Lee, M. K. Khaing Oo, and X. Fan, "Rapid, sensitive, and multiplexed on-chip optical sensors for micro-gas chromatography," Lab Chip (2011), doi:10.1039/C1032LC20922E.
8. H.- Noh, P. J. Hesketh, and G. C. Frye-Mason, "Parylene gas chromatographic column for rapid thermal cycling," J. Microelectromech. Syst. **11**(6), 718–725 (2002).
9. M. Agah, J. A. Potkay, G. Lambertus, R. Sacks, and K. D. Wise, "High-performance temperature-programmed microfabricated gas chromatography columns," J. Microelectromech. Syst. **14**(5), 1039–1050 (2005).
10. S. C. Terry, J. H. Jerman, and J. B. Angell, "A gas chromatographic air analyzer fabricated on a silicon wafer," IEEE Trans. Electron. Dev. **26**(12), 1880–1886 (1979).
11. G. R. Lambertus, C. S. Fix, S. M. Reidy, R. A. Miller, D. Wheeler, E. Nazarov, and R. Sacks, "Silicon microfabricated column with microfabricated differential mobility spectrometer for GC analysis of volatile organic compounds," Anal. Chem. **77**(23), 7563–7571 (2005).

12. S. Reidy, D. George, M. Agah, and R. Sacks, "Temperature-programmed GC using silicon microfabricated columns with integrated heaters and temperature sensors," Anal. Chem. **79**(7), 2911–2917 (2007).
13. E. T. Zellers, S. A. Batterman, M. Han, and S. J. Patrash, "Optimal coating selection for the analysis of organic vapor mixtures with polymer-coated surface acoustic wave sensor arrays," Anal. Chem. **67**(6), 1092–1106 (1995).
14. E. Özkumur, J. W. Needham, D. A. Bergstein, R. Gonzalez, M. Cabodi, J. M. Gershoni, B. B. Goldberg, and M. S. Unlü, "Label-free and dynamic detection of biomolecular interactions for high-throughput microarray applications," Proc. Natl. Acad. Sci. U.S.A. **105**(23), 7988–7992 (2008).
15. P. C. Beard, "Interrogation of free-space Fabry–Perot sensing interferometers by angle tuning," Meas. Sci. Technol. **14**(11), 1998–2005 (2003).
16. Y. Hou, S.-W. Huang, S. Ashkenazi, R. Witte, and M. O'Donnell, "Thin polymer etalon arrays for high-resolution photoacoustic imaging," J. Biomed. Opt. **13**(6), 064033 (2008).

1. Introduction

The Fabry-Pérot (FP) cavity holds great promise in developing on-chip miniaturized sensor arrays for non-destructive, rapid, and sensitive vapor detection [1–7]. It is particularly attractive for on-column sensing applications in micro-gas chromatography (µGC), as it is highly compatible with microfluidics [3,4, 6,7]. An FP vapor sensor consists of a vapor sensitive polymer coated on a solid substrate (*e.g.*, silicon wafer or glass slide). As shown in Fig. 1, light reflected from the air-polymer interface and polymer-substrate interface forms an interference pattern. The interaction between the polymer and vapor analyte causes a change in the polymer thickness and refractive index (RI), which in turn results in a change in the reflection spectrum (Fig. 1(B)). Thus, by measuring the reflection spectrum shift, the change in the polymer thickness and RI, and hence the concentration of the analyte, can be quantified. Usually such spectral domain measurements involve a bulky spectrometer, and are often slow and limited by the spectral resolution of the spectrometer. A tunable diode laser has also been employed to measure the FP sensor spectral shift [3]. While providing a high spectral resolution, the tunable diode laser is expensive and has a limited tuning speed and range.

A third method is to fix the incident laser wavelength at a quadrature point of the FP interference spectrum and then monitor the light intensity change (see Fig. 1(B)) [4, 6,7]. This method is simple, fast, sensitive, and amenable to integration of all components (light source, sensor, and detector) on a single chip. However, in practice, the light intensity measurement method encounters a hurdle. While most experimental conditions can be controlled precisely, the thickness of the polymer layer, which is usually deposited on a solid substrate through drop-coating, dip-coating, or spin-coating, may vary significantly from batch to batch. Such variations adversely cause the detection wavelength to deviate from the most sensitive quadrature point and thus results in different detection sensitivities that negate analyte quantitation. This problem is exacerbated when an array of sensors is employed with different polymer coatings that may have different thicknesses (and different RIs, as well) [6,7]. Simultaneously achieving the optimal detection conditions for all those sensors becomes virtually impossible.

Here, we develop a self-referenced composite FP cavity sensor that enables precise measurement of the change in the polymer thickness and RI, and hence quantification of analytes, without prior knowledge of the polymer thickness. The composite
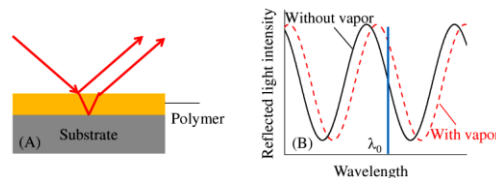

Fig. 1. (A) Side view of an on-chip Fabry-Pérot (FP) sensor. Absorption of analytes by polymer results in a change in thickness and/or refractive index of the polymer, which in turn leads to a change in the characteristic FP spectrum as shown in (B). The shift in the spectrum can be measured as a change in reflected intensity at a fixed wavelength.
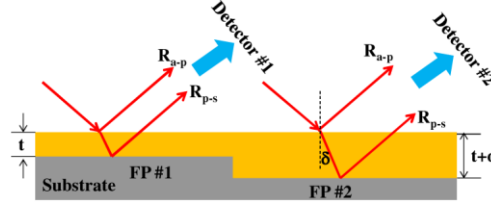
Fig. 2. Schematic of the self-referenced composite FP sensor.

FP is illustrated in Fig. 2. It is formed by two juxtaposed independent FPs with a slight polymer thickness offset. Although the polymer thicknesses (t and t+d in Fig. 2) are unknown, the offset (d in Fig. 2) can be precisely controlled during the fabrication, thus allowing us to accurately extract the change in the polymer thickness and RI upon exposure to the vapor analyte. This design retains all the benefits of standard single FP sensors, including ease of fabrication and implementation, excellent compatibility with micro-gas chromatography (µGC) components [8–12], and rapid detection of analytes, while providing several significant advantages. First, the composite FP is able to precisely measure the thickness and RI change of the polymer, regardless of the polymer thickness, RI, and light incident angle and wavelength, thus enabling accurate vapor quantitation. Second, the detection becomes much more flexible, as nearly any wavelength and incident angle can be used without the need for precisely interrogating the sensor at a quadrature. Third, since the composite FP provides the actual change in polymer thickness and RI, it has a larger dynamic range, as compared to the measurement at a quadrature.

In this paper we first discuss the underlying detection theory, and report the fabrication and characterization of the composite FP sensor. Then the tests of the composite FP sensor are performed under the pulsed vapor analyte flow at two different light incident angles. Rapid and consistent measurement of the polymer changes is achieved with three different analytes of various concentrations. The detection limit is found to be on the order of a few pico-grams.

2. Theory

Referring to Fig. 2, the reflected light intensity at FP #1 is given by:

$$I_1(\lambda) = R_{a-p} + R_{p-s} + 2 \times \sqrt{R_{a-p}R_{p-s}} \cos\phi, \qquad (1)$$

where $R_{a\text{-}p}$ and $R_{p\text{-}s}$ are the reflectivity at the air-polymer interface and polymer-substrate interface, respectively. $\phi = 4\pi \cdot n \cdot t \cdot \cos\delta / \lambda$, where n and t are the polymer RI and thickness, respectively. δ and λ are the incident angle in the polymer and the wavelength in vacuum, respectively. The light intensity change caused by the vapor-polymer interaction is described by:

$$\Delta I_1 = -8\pi \cos\delta / \lambda \times \sqrt{R_{a-p}R_{p-s}} \sin(\phi)\Delta(nt), \qquad (2)$$

In vapor sensing applications, $\Delta(nt)$ can be used to quantify the analyte. However, in a regular FP sensor, since the polymer thickness (and hence ϕ) varies significantly, relating the intensity change, ΔI_1, to $\Delta(nt)$ becomes quite challenging.

This obstacle can be overcome by introducing another FP sensor, adjacent to the first one, with an additional thickness, d. Similar to Eq. (2) and under the assumption that the vapor causes the same polymer response ($\Delta(nt)$) in FP #2, we have,

$$\Delta I_2 = -8\pi \cos\delta / \lambda \times \sqrt{R_{a-p}R_{p-s}} \sin(\varphi + \theta)\Delta(nt), \qquad (3)$$

where $\theta = 4\pi \cdot n \cdot d \cdot \cos\delta / \lambda$. From Eqs. (1) - (3), we obtain:

$$\Delta(nt) = A \frac{\sqrt{(\Delta I_1)^2 + (\Delta I_2)^2 - 2\cos\theta \cdot \Delta I_1 \cdot \Delta I_2}}{\sin\theta}, \tag{4}$$

where A is a constant that contains the information about the light incident angle, wavelength, reflectivities at the two interfaces, and the detector responsivity. Note that, in Eq. (4), $\Delta(nt)$ is no longer dependent upon the polymer thickness, t, but only the polymer thickness difference, d. As shown later, d, can be created through the micro/nanolithographic method with high precision and high reproducibility. Therefore, $\Delta(nt)$ can be obtained uniquely by measurement of the reflected light intensity change at the two sensors, thus enabling rapid and accurate quantification of the vapor analyte. Also note that in the above derivation, we assume that the vapor causes the same polymer response (*i.e.,* $\Delta(nt)$) in both FP #1 and #2. This is true when the vapor is in the pulsed format and the exposure time of the polymer to the vapor is short so that only the superficial layer of polymer is affected.

3. Experimental

3.1 Sensor preparation

The fabrication procedure for the composite FP is illustrated in Fig. 3(A). The prime grade silicon wafers are spin-coated with a photoresist and lithographically patterned using an MA-6. The wafers are then etched using a Pegasus deep reactive ion etching (DRIE) tool (etch depth, d=1.3 μm). The etched wells are 400 μm long and 200 μm wide. The first layer of photoresist is removed, and the wafer is then recoated with photoresist and patterned with precise alignment using the MA-6. The wafers are once again etched using the DRIE tool (etch depth, t=1 μm). The resulting etched area is 400 μm long and 400 μm wide, and is aligned to overlap with the previously etched area. This results in a staggered etch, with half of the total etched area etched to a depth of 2.3 μm and the other half etched only 1 μm (Fig. 3(B)). The resultant silicon wafer is then diced into 8 mm x 10 mm pieces using an ADT 7100 dicing saw. These pieces are immersed overnight in sulfuric acid-dichromate solution to oxidize any contaminants, followed by a rinse with deionized water, and finally placed under
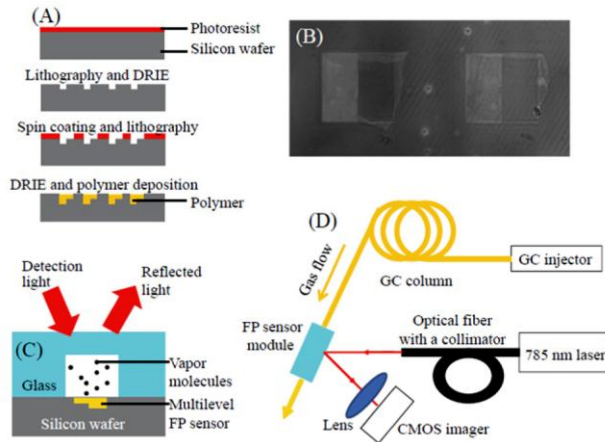

Fig. 3. (A) Fabrication of a composite FP sensor. The sensors are fabricated using a two-step lithography and deep reactive etching process. Polymers are spin-coated or drop-coated on the wafer. (B) Image of the composite FP sensor acquired using a CMOS imager. Each well is 400 μm long and 200 μm wide. The depth offset (*i.e.*, d in Fig. 2) is 1.3 μm. (C) Cross-sectional view of the composite FP sensor on a silicon substrate enclosed by an open-bottom glass microfluidic channel (1 mm deep and 600 μm wide). (D) Schematic of the experimental setup.

UV light for an hour to ensure removal of any residues. Then OV-215 (Ohio Valley Specialty, 1057) is chosen as the vapor sensing layer, as it is a commonly used in many GC applications and vapor sensors [7, 13]. The polymer solution is prepared by dissolving the

polymer gum in ethyl acetate (OV-215:ethyl acetate = 1:3 in mass). The polymer is then coated using a spin coater to achieve a smooth layer. The polymer solution is first spun at 1,300 rpm for 10 seconds and then at 6,000 rpm for 30 seconds. The spin-coated chip is subsequently heated for 60 seconds at 60 °C to completely remove the solvent. Finally, an open-bottom microfluidic channel assembled from glass slides and UV-curable optical glue is used to seal the silicon chip (Fig. 3(C)). The resulting channel is approximately 1 mm deep and 600 μm wide.

3.2 Experimental setup

The experimental setup is illustrated in Fig. 3(D). Analytes are injected using a standard GC injection port and the analyte in the pulsed format is then delivered to the sensor via a 4 m long GC guard column (inner diameter: 250 μm). The detection beam from a Toptica 785 nm laser is aligned using an FC/APC terminated optical fiber and a beam collimator. A Thorlabs CMOS imager, with an acquisition rate of 16 frames per second, is used to acquire the light reflected from each FP sensor through a lens (Edmund Optics, VZM450). The precise and instantaneous transduction signal from the FP sensor is captured for post-analysis. All experiments are carried out at room temperature. Mass of the injected analytes is calibrated using a mass spectroscopy system. Helium is used as the carrier gas with a flow rate of 8 mL/min.

4. Results

In the experiment, we choose to use two different incident angles, 21° and 26°, to intentionally create a situation that deviates from the traditional quadrature detection. The temporal response of each individual sensing element (FP #1 and #2 in Fig. 2) of the composite FP sensor is shown in Fig. 4. Introduction of analyte from the GC injection port leads to a rapid rise in the measured signal, corresponding to the shift in the interference spectrum. This increase is attributed to the change in polymer thickness and RI as the analyte is absorbed by the polymer. Subsequently, the gas flow in the GC and microfluidic column rapidly purges the analyte from the polymer, resulting in a rapid decline back to the baseline in the measured signal. The chromatograms reveal a sub-second response time when each individual FP sensing element is interrogated at both 21° and 26° angles of incidence. However, comparison among Fig. 4(A)-(D) shows the strong influence of polymer thickness and angle of incidence on the sensor response to the injected vapor analyte. According to Fig. 4(A) and (B), at 21° incident angle, FP #1 has a peak height of 25, while FP #2 has a peak height of 16.5. This difference is due to the different thickness of polymer layer in each individual FP sensing element. Similar difference (28 counts vs. 15 counts) can also be found for FP #1 and #2 at 26° incident angle, as shown in Fig. 4(C) and (D). Likewise, different incident angles also cause different sensitivities even in the same FP sensor due to the slight
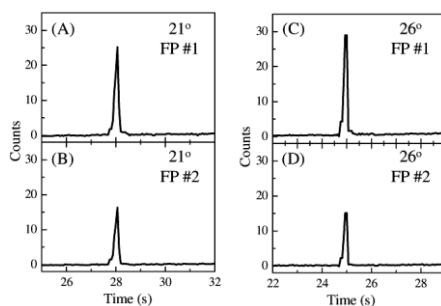

Fig. 4. Response of individual FP sensing elements in the composite FP sensor to 5 ng of acetone at the incident angle of 21° and 26°. In all cases the sensors demonstrate a rapid response time in the sub-second range. $\Delta(nt)$ at 21° is 12.51 and $\Delta(nt)$ at 26° is 12.48, based on Eq. (4) (assuming that A = 1 in Eq. (4)).

light path difference in the polymer. These variations highlight the difficulties in obtaining accurate quantitation of the vapor analyte.

In contrast, by using the information gained from the self-referenced composite FP sensor (*i.e.,* both FP #1 and #2), $\Delta(nt)$ can be calculated very precisely. Based on Eq. (4), $\Delta(nt)$ in Fig. 4 is 12.51 and 12.48 for the 21° and 26° incident angle, respectively, which represents a variation of only 0.3%. Figure 5 presents the calculated $\Delta(nt)$ at 21° and 26° for three different vapor analytes, acetone, heptane, and toluene, at various injected masses. It clearly shows that for each analyte the calculated $\Delta(nt)$ is nearly equal at both angles of incidence across the entire range of injected mass. Therefore, $\Delta(nt)$ can be used for analyte quantitation regardless of the polymer thickness or incident angle (Note: for some angles at which $\sin(\theta) = 0$, our approach becomes invalid). Linear response is obtained when the injected mass is below approximately 4 ng. At higher injected masses, $\Delta(nt)$ levels off due to the polymer saturation. Additionally, these sensors maintain the high sensitivity and low detection limits previously reported. Given the noise level of 0.38, the detection limit for acetone, heptane, and toluene is about 5.7 pg, 9 pg, and 11 pg or, based on the retention time (~4 s) and the peak width (0.125-0.15 s), as well as the inner diameter and length of the GC column, which correspond to approximately 200 ppb, 335 ppb, and 405 ppb in concentration, respectively [7]. These results are comparable to the best results demonstrated by traditional single FP sensors under the optimal quadrature detection condition [7].
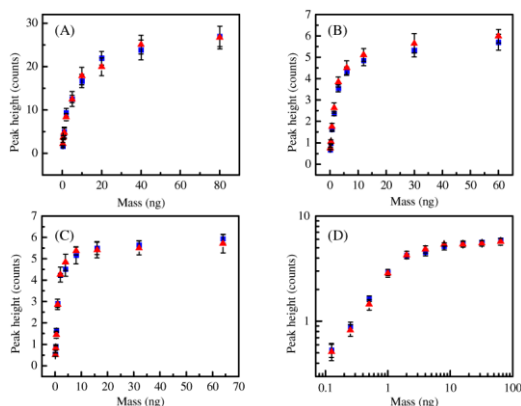

Fig. 5. Response of sensors at 21° (squares) and 26° (triangles) to various injected masses of (A) acetone, (B) heptane, (C) toluene. (D) Log-log plot corresponding to (C). Error bars are obtained from 5 tests.

5. Conclusion

We have developed a self-referenced composite FP vapor sensor to overcome the sensitivity variations caused in batch to batch processing of polymers. The sensor provides accurate measurement of the change in polymer thickness and RI, thus enabling vapor quantitation. The sensor can be used with nearly any polymer thickness, RI, and light incident angle and wavelength. These advantageous features, coupled with the use of a single optical source and single optical detector (CMOS imager), make the composite FP sensor a promising technology platform in various applications, including vapor sensing as demonstrated in the current paper, pressure sensing, protein detection [14], and photo-acoustic imaging [15, 16].